A new Rossby Wave-breaking interpretation of the North Atlantic Oscillation

Article

Published Version

A New Rossby Wave–Breaking Interpretation of the North Atlantic Oscillation

TIM WOOLLINGS AND BRIAN HOSKINS

Department of Meteorology, University of Reading, Reading, United Kingdom

MIKE BLACKBURN AND PAUL BERRISFORD

Walker Institute, Department of Meteorology, University of Reading, and National Centre for Atmospheric Science, Reading, United Kingdom

(Manuscript received 14 November 2006, in final form 23 April 2007)

ABSTRACT

This paper proposes the hypothesis that the low-frequency variability of the North Atlantic Oscillation (NAO) arises as a result of variations in the occurrence of upper-level Rossby wave–breaking events over the North Atlantic. These events lead to synoptic situations similar to midlatitude blocking that are referred to as high-latitude blocking episodes. A positive NAO is envisaged as being a description of periods in which these episodes are infrequent and can be considered as a basic, unblocked situation. A negative NAO is a description of periods in which episodes occur frequently. A similar, but weaker, relationship exists between wave breaking over the Pacific and the west Pacific pattern.

Evidence is given to support this hypothesis by using a two-dimensional potential-vorticity-based index to identify wave breaking at various latitudes. This is applied to Northern Hemisphere winter data from the 40-yr ECMWF Re-Analysis (ERA-40), and the events identified are then related to the NAO.

Certain dynamical precursors are identified that appear to increase the likelihood of wave breaking. These suggest mechanisms by which variability in the tropical Pacific, and in the stratosphere, could affect the NAO.

1. Introduction

As shown by Pelly and Hoskins (2003), the onset of midlatitude blocking episodes is associated with the breaking of upper-level Rossby waves. Recently Benedict et al. (2004) suggested that a similar wave-breaking process is responsible for the variations associated with the North Atlantic Oscillation (NAO). The synoptic evolution they associate with negative NAO anomalies is particularly similar to blocking, but occurs at higher latitudes on the poleward side of the storm track. In this paper we further investigate the relationship between these blocking-like events and the NAO.

As discussed in Berrisford et al. (2007), the term "blocking" is generally used to describe an atmospheric phenomenon in which a large, quasi-stationary anticyclone develops in the midlatitudes and persists for several days or longer, blocking the ambient westerly winds and weather systems. However, there is a wide range of anticyclonic activity seen in the midlatitude atmosphere, and there is currently no consensus on exactly what type of system should be classified as a block. Objective analyses that try to identify distinct weather regimes frequently turn up patterns with an anticyclone lying on the poleward side of the storm tracks. In the Atlantic these occur in the vicinity of southern Greenland, as a so-called Greenland blocking regime (Cheng and Wallace 1993; Vautard 1990; Kimoto and Ghil 1993). Similar behavior is seen in the Pacific sector in the "Alaska Ridge" of Cheng and Wallace (1993).

When anticyclones such as these lie just off the storm track and jet stream locations, their effect is more to divert the ambient westerly flow than to block it. They are, however, often identified as blocks by objective blocking indices. Generally such indices have focused on a particular band of latitude, for example, a constant latitude in Tibaldi and Molteni (1990) and the varying latitude of the storm track maximum in Pelly and Hoskins (2003). In these studies the picture is dominated by

Corresponding author address: Tim Woollings, Department of Meteorology, University of Reading, Earley Gate, P.O. Box 243, Reading RG6 6BB, United Kingdom.
E-mail: t.j.woollings@rdg.ac.uk

DOI: 10.1175/2007JAS2347.1

blocking over Europe and the east Pacific. Recently, however, Schwierz et al. (2004), Scherrer et al. (2006), and Diao et al. (2006) have all developed two-dimensional indices that search for blocking at all latitudes, and these show more significant occurrence of blocking at high latitudes in both ocean basins. Berrisford et al. (2007) extended the Pelly and Hoskins index to a two-dimensional index in order to study blocking at various latitudes in the Southern Hemisphere. They found frequent occurrence of blocking-like episodes associated with wave breaking at high latitudes, and referred to these as "high-latitude blocking" in order to distinguish them from midlatitude blocks that clearly do block the westerly winds and storms, rather than divert them. We will use the same terminology here.

Several studies have uncovered a clear link between high-latitude blocking in the Atlantic sector and the NAO, with much more frequent blocking during the negative phase of the NAO (Shabbar et al. 2001; Luo 2005; Scherrer et al. 2006). The NAO is the dominant pattern of atmospheric variability over the Atlantic (e.g., Wallace and Gutzler 1981; Hurrell 1995), and as such has been the subject of much research (see, e.g., the review by Wanner et al. 2001). The NAO exhibits variability on all time scales, but several recent studies have focused on synoptic time scales in attempts to explain the underlying dynamics (e.g., Vallis et al. 2004; Löptien and Ruprecht 2005).

In particular, Benedict et al. (2004) identified "NAO events" on the synoptic time scale, concluding that the breaking of upper-level Rossby waves was responsible for the NAO anomalies, with anticyclonic breaking leading to a positive NAO event and cyclonic breaking leading to a negative event. This process of wave breaking leading to NAO events has been simulated by perturbing a primitive equation model with perturbation patterns derived from Pacific storm track variations (Franzke et al. 2004).

This prompts us to reexamine the question of what exactly is the relationship between high-latitude blocking over the Atlantic and the NAO. It has been proposed that the negative NAO phase acts as a preconditioning so that the formation of a persistent anticyclone is more likely when the atmosphere is in this state. This preconditioning could occur through a modification of the planetary stationary waves in response to the surface temperature anomalies associated with the negative NAO, as has been suggested by Shabbar et al. (2001), Huang et al. (2006), and Barriopedro et al. (2006), or by the tendency for a more diffluent jet during the negative NAO phase, as suggested by Luo (2005). Alternatively, it could be proposed that the blocking influences the NAO, in line with the suggestion of Croci-Maspoli et al. (2007) that Atlantic blocking events can trigger the onset of the negative NAO phase. There is also a third possibility, suggested by the synoptic view of the NAO outlined above, that the negative NAO and high-latitude blocking over the Atlantic are simply two different descriptions of the same phenomenon. This would be consistent with the simple model of Luo et al. (2007), and also with the suggestion of Berrisford et al. (2007) that wave-breaking episodes in certain regions of the Southern Hemisphere are a local manifestation of the Antarctic Oscillation.

Here we investigate this issue by applying the two-dimensional potential-vorticity-based index of Berrisford et al. (2007) to data from the 40-yr European Centre for Medium-Range Weather Forecasts (ECMWF) Re-Analysis (ERA-40). This index identifies high-latitude blocking events in both the Atlantic and Pacific sectors that are very similar. Teleconnection indices are used to show that there is, indeed, a very close link between the Atlantic events and the NAO and that a similar relationship holds between events in the Pacific and a pattern of low-frequency variability referred to as the "West Pacific Pattern" (WPP). We also composite the high-latitude blocking events to examine the anomalies associated with them and to identify anomalies preceding them, which could indicate dynamical precursors.

2. Methodology

The data used in this study are from ERA-40 (Uppala et al. 2005), from which data from December 1957 to December 2001 were available. Only events in the winter period of December–February (DJF) are examined, though note that a few days in November and March are necessarily included when compositing the periods before, or after, an event. All the data used here has the full ERA-40 resolution of 1.125°.

In recognition of the importance of upper-level Rossby wave breaking in blocking episodes, the Pelly and Hoskins (2003) blocking index searches for a reversal of the meridional gradient of potential temperature θ on the dynamical tropopause, defined as the potential vorticity (PV) surface at 2 PVU. Here we extend this index simply by applying it at all latitudes from 25° to 73°N, as in Berrisford et al. (2007), rather than just at the latitude of maximum transient eddy kinetic energy. In general then, we refer to this as a wave-breaking rather than a blocking index, again following Berrisford et al. Apart from this, all parameters and definitions are the same as those used to define blocking episodes by Pelly and Hoskins (2003).

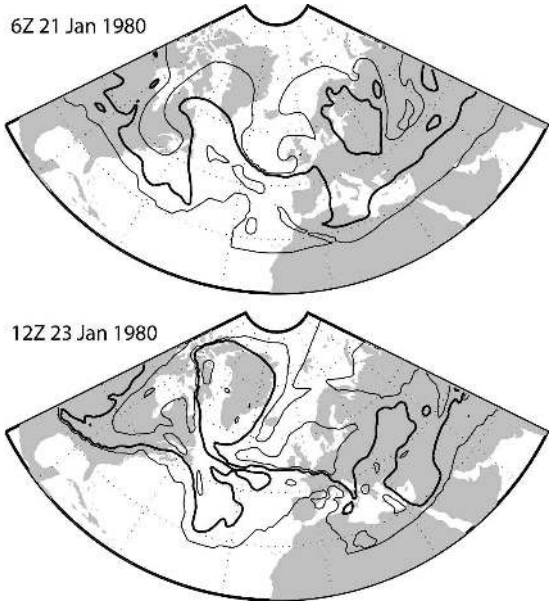

FIG. 1. An example of a Rossby wave-breaking event that leads to high-latitude blocking. This shows potential temperature on the 2-PVU surface contoured at 300, 315 (bold), and 330 K.

The index is calculated at every point on a grid of spacing 4° in latitude and 5° in longitude. Potential temperature is averaged over two boxes of 5° longitude and 15° latitude, one on the poleward side of the point and the other on the equatorward side. An instantaneous wave-breaking index at this central point is defined as the poleward value minus the equatorward value, so that this index is positive if the gradient is reversed. To separate out the largest and most persistent events, several spatial and temporal constraints are then applied, as follows. Any latitudinal movement of the pattern is accounted for by simply taking the maximum of the instantaneous index over ±4° of latitude. We define large-scale wave breaking to be an event where the instantaneous index is positive for at least 15° of longitude and then a wave-breaking episode is identified at a given point if large-scale wave breaking occurs within 10° of longitude of that point for five consecutive days. These criteria ensure that the episodes selected by this index have a significant zonal and meridional extent, persist for at least 5 days, and are quasi stationary.

An example of the type of event identified by this index is shown in Fig. 1. The top panel shows θ_{PV2} on the onset day of an episode in January 1980. At this time there is a clear cyclonic overturning of contours over the western Atlantic. There is also a cutoff region of potentially warm air over northern Europe, which is the remnant of a European blocking event. Two days later (bottom panel) it is evident that a large mass of potentially warm, subtropical air has been advected poleward during the wave breaking. This air mass is now lying far to the north, over Greenland, where it acts as an anticyclonic anomaly. As a result of this, the air mass is beginning to turn anticyclonically and is only connected to the subtropics via a thin filament of high θ air. The potentially cold air on the southern flank of the wave breaking shows less tendency to cut off.

3. Wave-breaking occurrence

Preferred locations of wave breaking seen by this index are identified by calculating the episode frequency, simply the fraction of DJF days during which a given point is considered part of a wave-breaking episode. This is plotted in the left panel of Fig. 2. The well-known region of frequent blocking over Europe is

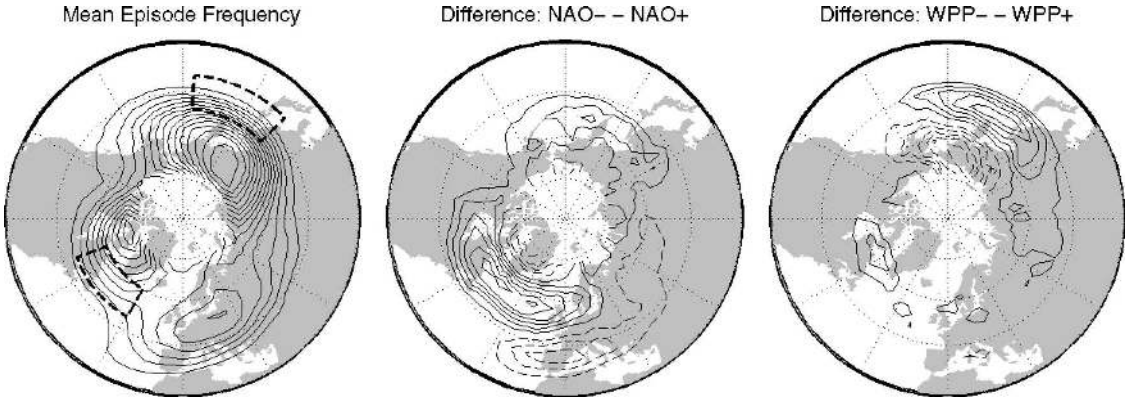

FIG. 2. (left) Wave-breaking episode frequency calculated for all DJF months in this study. This is the fraction of all DJF days considered part of a wave-breaking episode. The dashed lines mark the regions over which events are composited in the following sections. (middle),(right) The difference in episode frequency between negative and positive months of the NAO and WPP. The contour interval is 0.05, negative contours are dashed, and the zero contour is omitted.

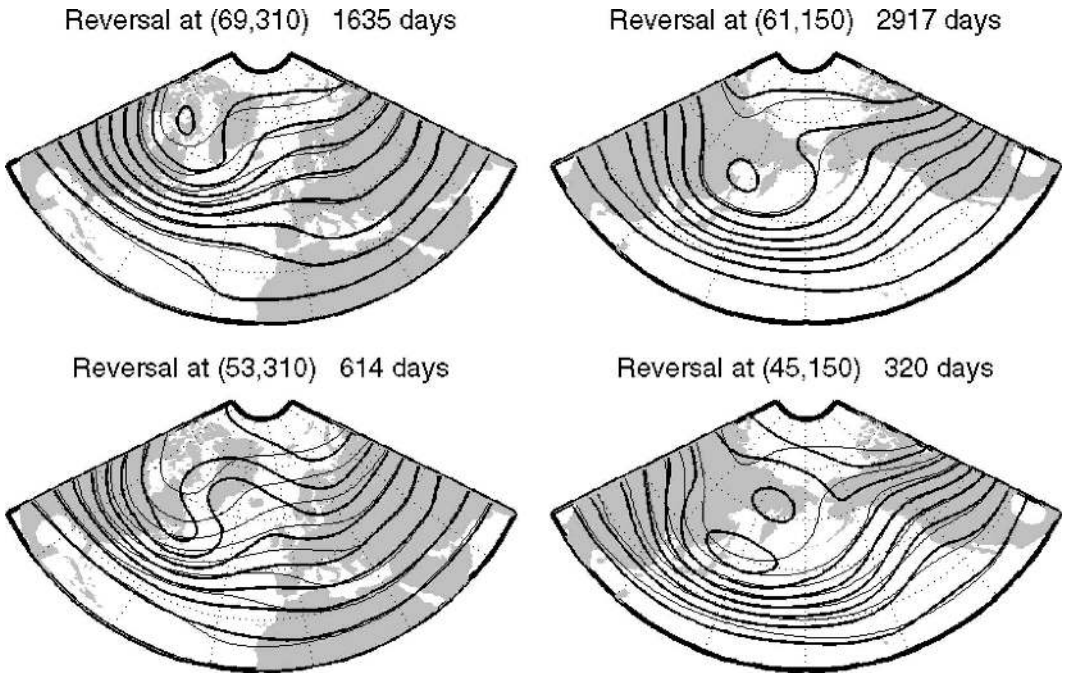

FIG. 3. Composites of 500-hPa geopotential height for all wave-breaking days that occur at a selection of points in the (left) Atlantic and (right) Pacific sectors. The latitude at which the gradient reverses and the number of days included are shown at the top of each panel. The climatology is shown in thin contours; contour interval is 100 m.

clearly seen, but the overall pattern is dominated by large maxima at high latitudes, centered over Siberia in the Pacific sector and Baffin Island in the Atlantic sector.

To determine whether these are, in fact, dynamically significant events, composites were made of all days during which a wave-breaking episode occurred at some representative points. These points were located along the meridians 50°W and 150°E, which pass through the Atlantic and Pacific frequency maxima, respectively, and examples at two different latitudes are given in Fig. 3. The winter climatology (shown in thin contours) features large troughs also centered over Baffin Island and Siberia. In both sectors the events are clearly dominated by cyclonic wave breaking, which acts to distort the respective climatological trough. The northernmost events (top panels) are weak, resulting in only a slight deviation from the climatology. This is mostly because the climatological gradient is weak there, so easier to overturn, but could also be partly attributed to the index used, since at higher latitudes a box of 15° of longitude will cover a smaller area, so the criteria will be easier to satisfy.

Wave breaking occurs less frequently farther south (bottom panels), but these events result in much more significant anomalies. Even there, however, the classical cutoff dipole pattern, which is often associated with blocking, is only seen for lower-latitude events in the Pacific. This suggests a continuum of behavior, ranging from frequent weak events at very high latitudes to occasional strong events farther south. Only the most dramatic of these conform to the conventional interpretation of midlatitude blocking, so in general we will follow Berrisford et al. (2007) in referring to these as high-latitude blocking episodes (HLBEs).

To investigate the link between HLBEs and patterns of variability such as the NAO, we first derive some indices of low-frequency variability in the ERA-40 dataset. For this purpose we use the mean sea level pressure (MSLP) field, since it is most commonly associated with the NAO, and we follow the teleconnectivity approach of Wallace and Gutzler (1981). Monthly means of MSLP for the DJF months 1957–2001 were interpolated onto a regular 2.5° × 2.5° grid extending from 20°N to the pole, then normalized with the mean and standard deviation of the respective month, thus removing the seasonal cycle. The teleconnectivity at a point is then defined as the absolute value of the strongest negative correlation between the MSLP time series at that point and the MSLP time series at every other point. The resulting teleconnectivity map, corresponding to Fig. 7a of Wallace and Gutzler, is shown in Fig. 4. The strongest anticorrelations are those associated with the NAO, with values down to −0.74. In the Pa-

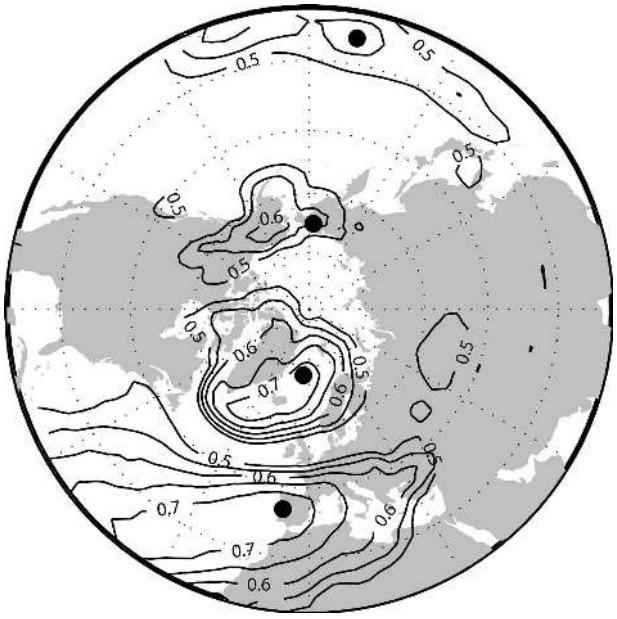

FIG. 4. Teleconnectivity of the Northern Hemisphere winter normalized monthly mean MSLP from ERA-40. The dots mark the points used to define the NAO and WPP indices. The contour interval is 0.05 with contours below 0.5 omitted.

cific there is an eastern and a western dipole, as seen by Wallace and Gutzler. The eastern dipole exhibits a slightly stronger anticorrelation, but this pattern is farther from the climatological trough, and after investigation appears to have a weaker relationship with episodes identified by the wave-breaking index. Following Wallace and Gutzler we refer to the western pattern as the WPP. The one-point correlation maps for the four centers marked in Fig. 4 are very similar to the corresponding maps of Wallace and Gutzler, and so are not shown here.

Indices for the NAO and WPP were derived by subtracting the normalized MSLP anomaly of the northern center from that of the southern center. A threshold of 0.5 standard deviations was then used to identify months characterized by the positive or negative phases of these patterns. This results in 43 positive and 45 negative NAO months and 47 positive and 41 negative WPP months.

The middle and right panels of Fig. 2 show the anomalies of wave-breaking episode frequency associated with the NAO and WPP, respectively, by plotting the episode frequency averaged over the negative months minus the episode frequency averaged over the positive months. These anomaly plots show a clear relationship between both patterns and the occurrence of wave breaking. There is a large increase in wave breaking in a wide swathe across the Atlantic during negative NAO months, when compared to positive months. A similar connection is seen with the WPP in the Pacific. In both cases the anomaly patterns take the form of meridional dipoles, with decreased frequencies farther north during negative months and increased frequencies there during positive months. This is easily understood by considering that, if the gradient is reversed during a wave-breaking episode, it is very unlikely to be reversed in the region around 30° farther north. There is also a signal centered over Spain that is associated with the NAO.

4. High-latitude blocking over the Atlantic

To determine the signature of HLBEs in various flow fields, all episodes occurring in a region of the western North Atlantic have been composited. By choosing a region in this way we are following the sector approach used in many blocking studies. The region chosen here is 50°–60°N, 30°–70°W and its boundary is shown by a heavy dashed line in the left panel of Fig. 2. This region is chosen to include the center of the NAO episode frequency anomaly maximum of Fig. 2, but does not extend past 30°W in order to avoid including European blocking events in the composites. Note that episodes in this region do result in significant anomalies, as shown in Fig. 3, and include, for example, the event illustrated in Fig. 1. If at least one point in this region is part of a HLBE, then an Atlantic HLBE is said to occur. For convenience we will refer to these as Greenland blocking episodes (GBEs). Onset days are defined as the first day considered as part of a GBE after 5 consecutive days that are not, and similarly decay days are defined as the last day considered as part of an episode before 5 days that are not. These criteria result in 1628 GBE days out of a possible 3991 DJF days (i.e., 41%), with 110 onset days and 107 decay days in the period.

Local flow patterns associated with GBEs are shown by plotting composites of various fields over all days during an episode and also during the periods 2–4 days before onset and 2–4 days after decay. All of these composites are shown as anomalies from the DJF mean, for simplicity, but note that almost identical patterns are obtained with a time-varying climatology. First, composites of θ_{PV2} are shown in Fig. 5. A very clear pattern is seen during the episodes, with a positive anomaly centered over Davis Strait. Characteristically this is associated with a large mass of anticyclonic air of subtropical origin that moved poleward during the wave-breaking event. South of this are two, more elongated anomalies that indicate an increased meridional gradient, suggesting a strong jet lying to the south of the

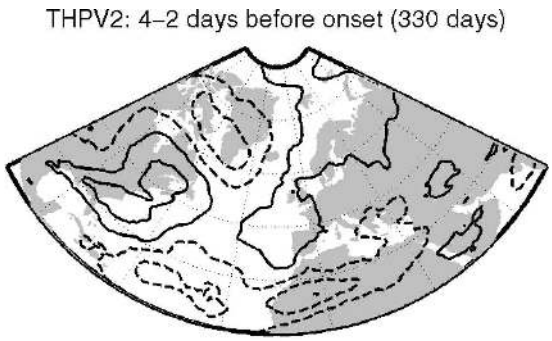

FIG. 5. Composites of θ_{PV2} anomalies before, during, and after high-latitude blocking episodes in the region 50°–60°N, 30°–70°W contoured at ±1, ±3, and ±5 K with negative contours dashed.

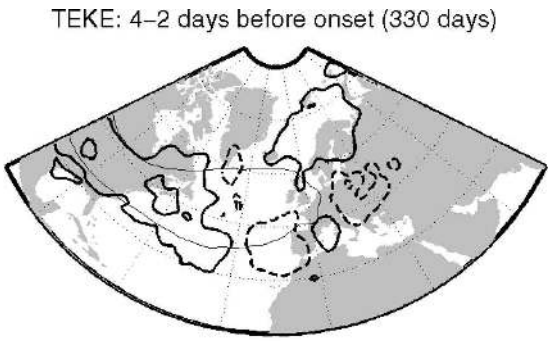

FIG. 6. As in Fig. 5 but for transient eddy kinetic energy at 250 hPa. The anomalies are contoured at ±5, ±15, ±25, and ±35 $m^2 s^{-2}$; the climatology is shown as a thin contour at 90 $m^2 s^{-2}$ for comparison.

anticyclonic anomaly. In the periods before onset and after decay the pattern appears reversed, but the anomalies are weaker and less coherent.

The behavior of the storm track is shown in Fig. 6 by plotting composites of the transient eddy kinetic energy (TEKE) at 250 hPa. This is derived from ERA-40 wind fields that have been filtered to retain only those parts which vary on time scales of 2–6 days (corresponding to the time scale of synoptic storms), using a Lanczos filter of length 60 days. Before onset there is anomalously strong storm activity across southern North America and at the start of the Atlantic storm track. The anomalous activity extends far south, suggesting that the transient eddies may play a role in the advection of warm subtropical air up to the poleward side of the jet. During GBEs there is a clear weakening of the Atlantic storm track, particularly on its downstream end and its poleward flank, showing that these events do act to divert transient weather systems. After decay there is an equally clear strengthening, especially on the equatorward side and extending into the Mediterranean. Taken together these equate to a southward shift of the storm track when averaged over the episode and the decay stage.

Figure 7 shows composites of the MSLP. During a GBE the pattern is very reminiscent of that associated with the negative NAO, while before onset, and especially after decay, it is more similar to the positive NAO anomaly pattern. The high pressure anomaly centered over Scandinavia before onset suggests that there may be a block over Europe in some cases. Figure 8 shows composites of the 2-m temperature. During an episode

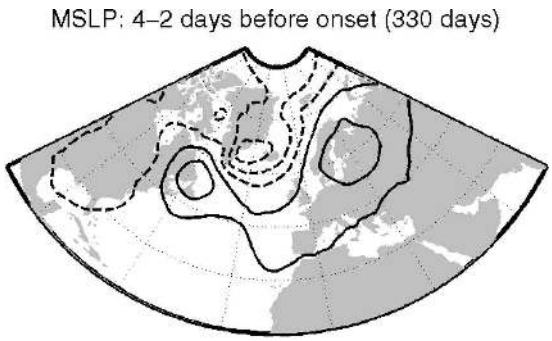

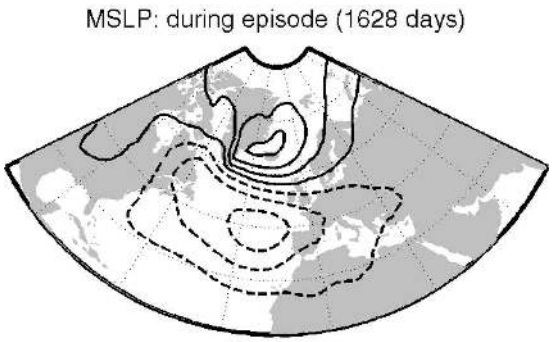

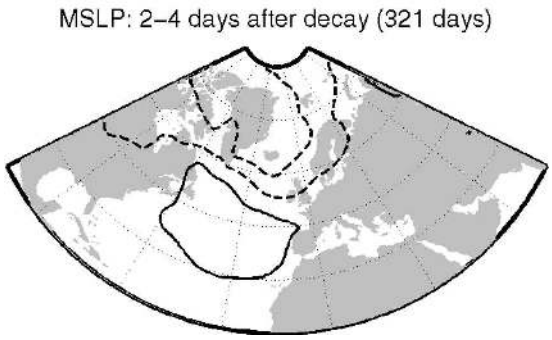

FIG. 7. As in Fig. 5 but for mean sea level pressure. Contours are drawn at ±1, ±3, ±5, and ±7 hPa.

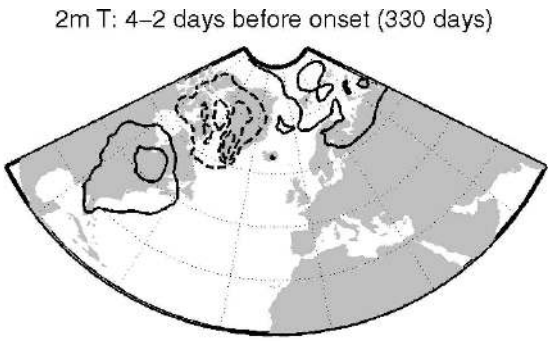

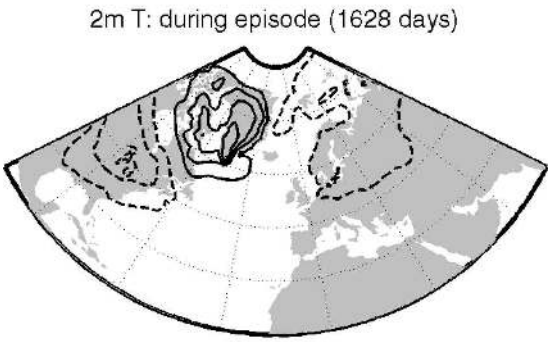

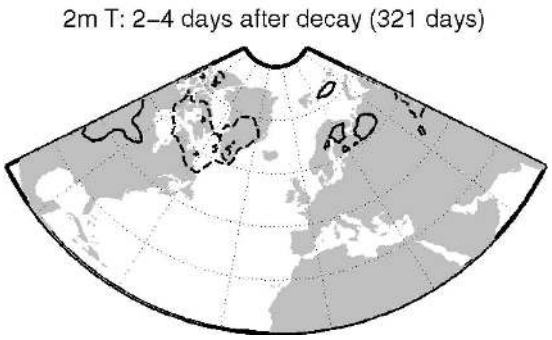

FIG. 8. As in Fig. 5 but for temperature at 2 m. Contours are drawn every kelvin with the zero contour omitted.

the temperature anomaly also resembles that associated with the negative NAO phase, with warmer conditions around Greenland and colder conditions around Scandinavia, as seen by van Loon and Rogers (1978). This anomaly pattern is consistent with the positive MSLP anomaly in Fig. 7, which would be associated with warm advection over Greenland and cold advection over Scandinavia. In the periods after decay and especially before onset, this temperature anomaly pattern is reversed.

These composites show that the signature of GBEs in a variety of atmospheric variables is very similar to the pattern associated with the negative phase of the NAO, but in the period immediately before the onset of these events the pattern is, if anything, reversed. This suggests that negative NAO anomalies do not act to precondition the flow so that wave breaking is more likely, but rather that negative NAO anomalies occur in association with GBEs.

To confirm this, the contribution of GBEs to the anomaly pattern of the negative NAO months was calculated. The monthly anomalies of MSLP, 2-m temperature, and 250-hPa streamfunction for the 45 negative NAO months are shown in the left panels of Fig. 9. The right panels show the same monthly anomalies after removing all days over which a GBE occurred. By removing these days the negative NAO pattern is almost entirely lost, confirming that this pattern is associated with GBEs. This is in agreement with Benedict et al. (2004), whose negative NAO events are identical to the GBEs described here. Note that there are only 460 days out of the 45 negative NAO months when there is

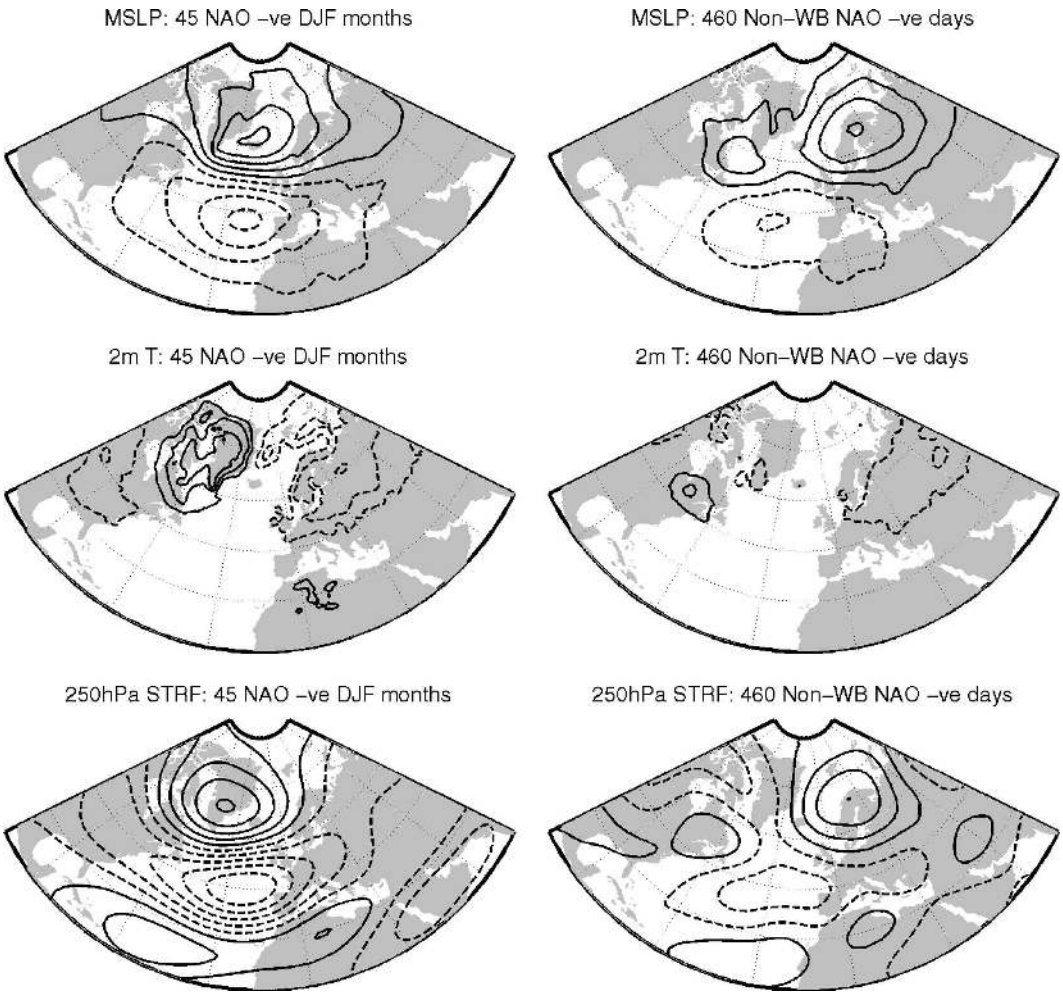

FIG. 9. (left) Anomalies of MSLP, 2-m temperature, and 250-hPa streamfunction generated by subtracting the winter climatology from the mean of the negative NAO months and (right) the same anomalies when all days featuring a high-latitude blocking episode in the region 50°–60°N, 30°–70°W have been removed from these months; contours are as in Figs. 7 and 8 for MSLP and temperature, and at ±1, ±3, ±5, ±7, and ±9 × 10^6 s^{-1} for the streamfunction.

not a GBE somewhere in this region, that is, only one-third of the total number of days in these months.

It is interesting to consider negative NAO anomalies from a synoptic PV perspective. During GBEs the surface high over Iceland is associated with the negative PV anomaly in the upper troposphere. The most likely source of this anomaly is advection from lower latitudes, as clearly occurs in the wave-breaking events described here. Middle-tropospheric heating associated with cyclones in the storm track to the south could have amplified the anomalies. A cold surface (produced by cooling or advection) could also be responsible for low-level anticyclonic circulation that could project onto the NAO pattern, but this is not observed during GBEs.

5. High-latitude blocking over the Pacific

Local flow patterns associated with Pacific HLBEs are seen by compositing episodes in the same manner as above but for the region 40°–50°N, 135°–175°E (shown in Fig. 2), which coincides with the positive anomaly in episode frequency during WPP months. These criteria result in 1676 Pacific HLBE days (i.e., 42% of the total) with 105 onset days and 96 decay days. Again, Fig. 3 shows that events here are dynamically significant. The signature of Pacific HLBEs in composites is very similar to that seen in the Atlantic, so they are not shown here. Instead, we simply assess the contribution of HLBEs to the WPP anomaly patterns, as above.

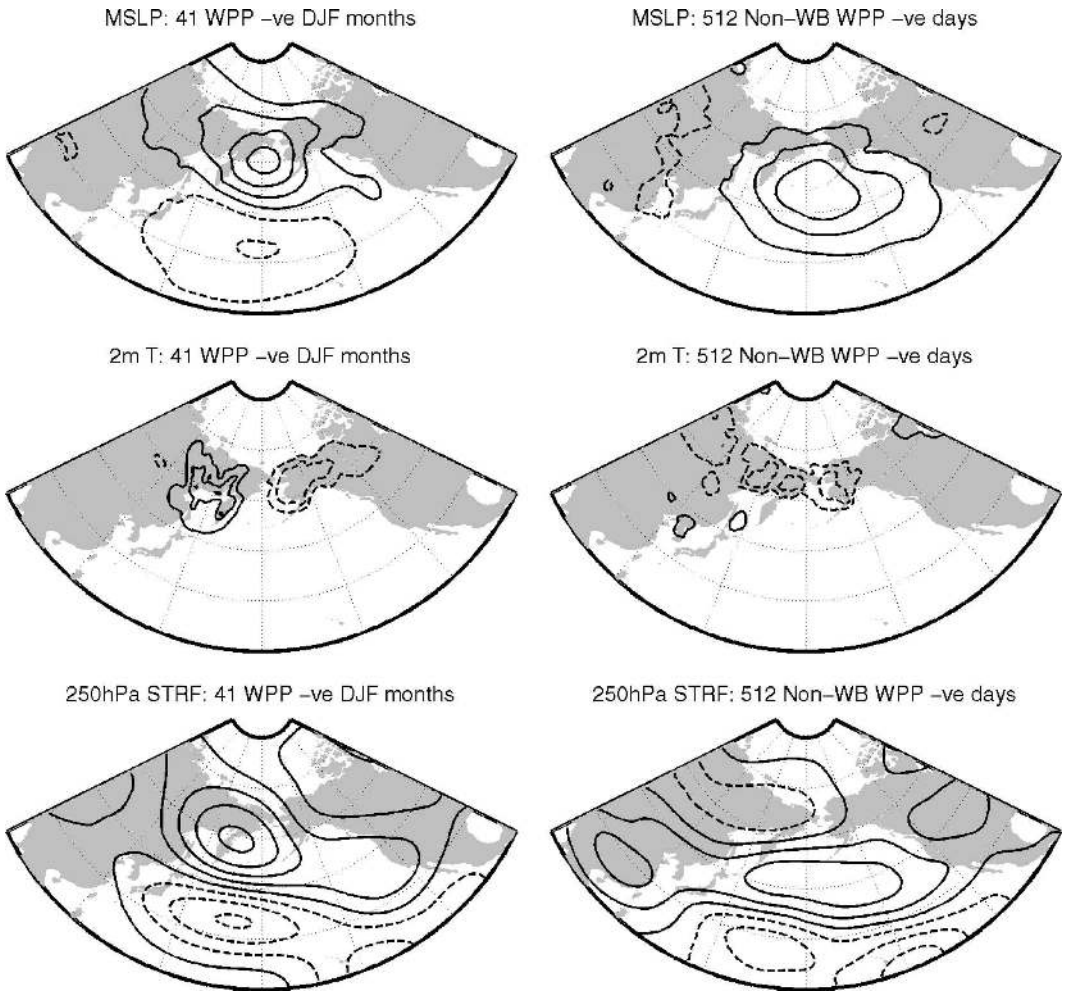

FIG. 10. As in Fig. 9 but for the WPP and high-latitude blocking in the region 40°–50°N, 135°–175°E.

The anomalies associated with negative WPP months are shown in the left panels of Fig. 10. These are very similar to the negative NAO pattern with an anticyclonic anomaly over the far north of the ocean basin and an east–west dipole in surface temperature as documented by Rogers (1981). As before, we then remove all days over which a HLBE occurred, and in the resulting anomalies, shown in the right plots, the characteristic pattern of the WPP is no longer seen. Instead, the pattern is of a weak Aleutian low and weak upper-level jet stream with no sign of a dipole in surface temperature. As in the Atlantic, the anomalies seen immediately before wave-breaking onset are more similar to positive WPP anomalies than negative ones (not shown). The conclusion is that, as before, negative WPP anomalies do not act to precondition the flow prior to the onset of a HLBE, but instead the negative WPP anomalies occur in association with HLBEs. It is interesting that, compared to the Atlantic, there are slightly more non-HLBE days and these are associated with a definite pattern.

6. The variability associated with HLBEs

We now investigate to what extent NAO and WPP variability is associated with variability in the occurrence of HLBEs. Beginning with the Atlantic we ask, specifically, how well can we estimate the NAO index in any given winter given only knowledge of the occurrence of GBEs? To answer this we calculate two time series: first, a winter NAO index obtained by differencing the normalized DJF mean pressures at the two centers found in the teleconnectivity analysis and, second, a GBE frequency series that is simply the number of GBE days in each winter. This second series is multiplied by -1 since we expect a high NAO index to be associated with a low occurrence of GBEs. Both series are normalized by their own means and standard de-

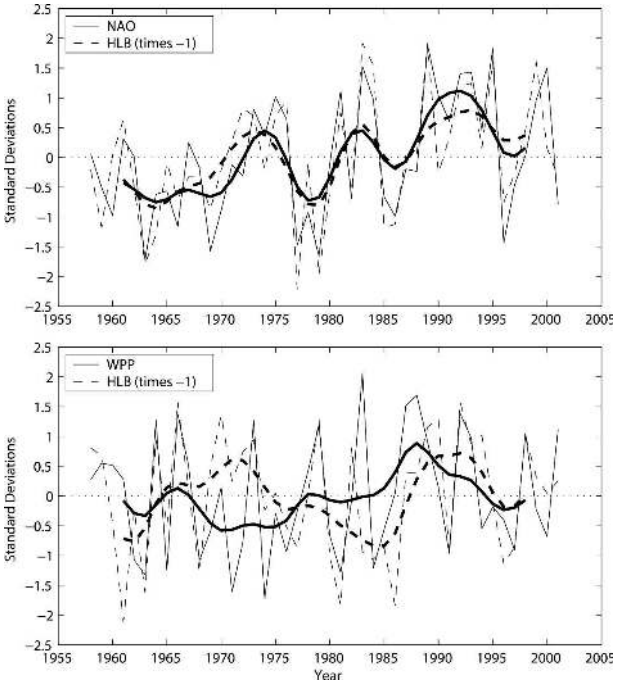

FIG. 11. (top) Time series of the winter NAO index in solid lines and the number of Greenland blocking episode days per winter in dashed lines. Both have been normalized and the thick lines show versions that have been smoothed using a low-pass filter with weights 1, 3, 5, 6, 5, 3, and 1. (bottom) As in (top) but for HLBEs in the Pacific and the WPP.

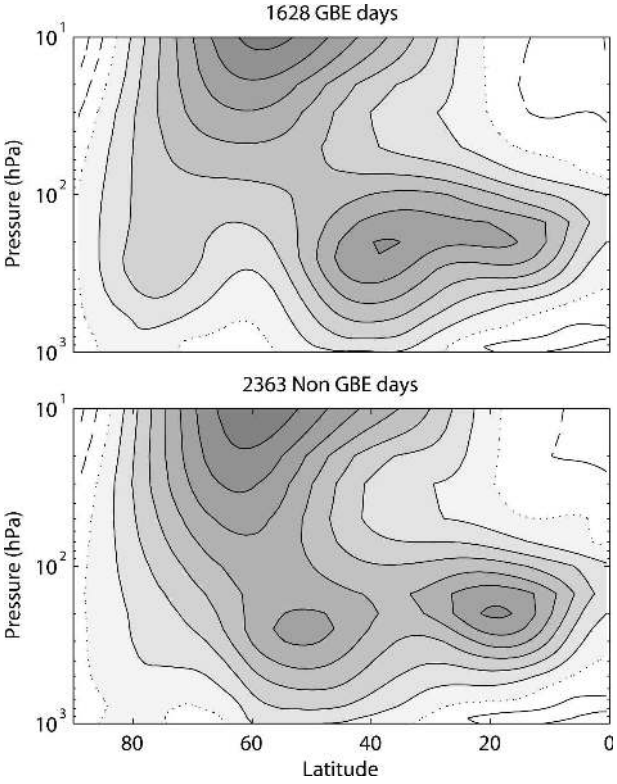

FIG. 12. Zonal mean wind averaged from 0° to 60°W over (top) all Greenland blocking episode days and (bottom) all remaining winter days. Contours are drawn every 5 m s^{-1} with negative contours dashed and the zero contour dotted.

viations, and are shown in the top panel of Fig. 11, along with versions that have been low-pass filtered to remove fluctuations with periods less than 4 yr, as in Hurrell (1995). There is clearly good agreement between the two series, with correlations of 0.84 between the unsmoothed and and 0.93 between the smoothed series. Most of the interannual, and almost all of the decadal NAO variability, is associated with variations in the occurrence of GBEs.

This motivates the central hypothesis of this paper: that the low-frequency variability exhibited by the NAO is a reflection of variations in the occurrence of GBEs, with NAO− corresponding to periods of frequent high-latitude blocking and NAO+ corresponding to periods when it is infrequent.

From this viewpoint, there are essentially just two different states of flow over the Atlantic. There is a basic, or unblocked, state and there is a blocked state. These two states are shown in Fig. 12 by plotting the zonal wind averaged over 0°–60°W for all GBE and non-GBE days. The basic, or non-GBE, state is characterized by well-separated subtropical and eddy-driven tropospheric jets at roughly 20° and 50°N, respectively. There is a strong stratospheric jet that connects down to the eddy-driven jet. In contrast, the blocked state features an area of weak zonal flow near 60°N, clearly a signature of the anticyclonic anomaly. The eddy-driven jet is diverted south around this anomaly so that it merges with the subtropical jet. The stratospheric jet is weaker and less connected to the tropospheric jet.

There are some obvious challenges to this interpretation. Are the episodes identified by this index actually dynamically different "events" in some way or just the tail end of the wind distribution? By counting the number of GBE days per year are we just estimating the mean zonal wind over the Atlantic, surely a very good NAO index?

Midlatitude blocking episodes are, however, known to exhibit different persistent characteristics, as shown by Pelly and Hoskins (2003), in that the probability of an event lasting one more day is larger if it has already lasted at least 5 days. Applying the same technique to the large-scale wave-breaking events over the Atlantic gives two distinct *e*-folding time scales of 2.1 days for events lasting 3 days or less and 3.3 days for those lasting 5 to 14 days (not shown; see Pelly and Hoskins for more details). This supports the impression that, while

shorter events simply reflect the passage of transient systems, longer events, or episodes, are associated with the irreversible deformation of PV contours leading to large-scale cutoff PV anomalies, which are often maintained by subsequent wave breaking. The temporal scales used here to define episodes ensure that only the latter, more persistent, events are selected.

The initial definition of the wave-breaking index requires that the meridional gradient of θ_{PV2} be reversed (i.e., greater than zero). If there was nothing "special" about wave breaking, then the threshold of zero would be considered arbitrary, and similar information regarding the distribution of zonal wind could be obtained by using any sensible threshold value. For example, all points where the difference between the northern and southern boxes is larger than 5 K could be identified and the same temporal and spatial scales applied in order to define episodes. The new time series of episode frequency could then be correlated with the NAO time series. The results of such an experiment are shown, in Fig. 13, for values of the threshold ranging from −10 to 10 K. While all thresholds from −5 to 5 K do result in high correlations, the maximum correlation is achieved with a threshold of zero, which is the point at which the index precisely indicates a reversal of the meridional gradient associated with wave breaking.

These results do, therefore, support the idea that, while the atmosphere exhibits a broad range of cyclonic and anticyclonic behavior, wave-breaking episodes do feature different dynamics. This justifies the conceptual separation of the flow into two general "states" (as in Fig. 12) that occur with similar frequency. Furthermore, it is these wave-breaking episodes, rather than simply strong or weak zonal flow in general, that are associated with most of the variability associated with the NAO.

We now assess the contribution of HLBEs to the variability associated with the WPP. The bottom panel of Fig. 11 compares the occurrence of HLBE days in the Pacific sector with the WPP index, as was done in the Atlantic. The full series have a correlation of 0.50, but the smoothed series are essentially uncorrelated (the correlation coefficient is 0.11). This shows that, while variations in the occurrence of HLBEs do have a clear effect on the WPP index from year to year, there are other processes affecting this index on the decadal time scale.

This is perhaps not surprising, given that other important large-scale patterns of variability exist in the Pacific, namely the El Niño–Southern Oscillation (ENSO) and the Pacific–North America (PNA) pattern. Although the WPP centers in Fig. 4 are local maxima in teleconnectivity, they are located only just to the west of the two westernmost PNA centers, and it does appear that the WPP index used here is affected by the PNA. Figure 10 shows that there is a clear pattern to the non-HLBE days in negative WPP months. This consists of a coherent high pressure anomaly extending across most of the North Pacific, which is very similar to the MSLP signal associated with the PNA (e.g., Wallace and Gutzler 1981, Fig. 18c). The evolution of the smoothed WPP index in Fig. 11 is also very similar to the evolution of the PNA over this period (see, e.g., the time series available online at http://www.cpc.noaa.gov). This suggests that the WPP index varies as a result of both HLBEs and the PNA and that the latter dominates on longer time scales. So, while variations in high-latitude blocking do have a significant effect on Pacific climate on the interannual time scale, their impact is of less importance than in the Atlantic.

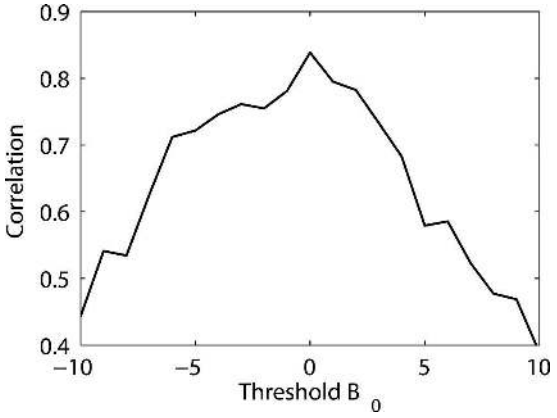

FIG. 13. Correlation of Atlantic wave-breaking frequency with the NAO, as in the thin lines of Fig. 11, as a function of the threshold parameter used in the wave-breaking index.

7. Precursors to high-latitude blocking

a. Atlantic events

We now examine the 110 GBE onsets for evidence of any consistent dynamical precursors to the wave breaking. The top panel of Fig. 14 shows a composite of 250-hPa streamfunction averaged over 2–4 days before onset for all cases. The time-averaged streamfunction generally highlights anomalies associated with the large-scale, low-frequency dynamics and does not suffer from a large mean gradient at low latitudes as seen in θ_{PV2}. Note that the anomalies used here have been normalized using the mean and standard deviation for the respective calendar month. This composite shows a large anticyclonic anomaly over northern Europe, consistent with the impression that GBEs may often be preceded by blocking over Europe. There is also a wave

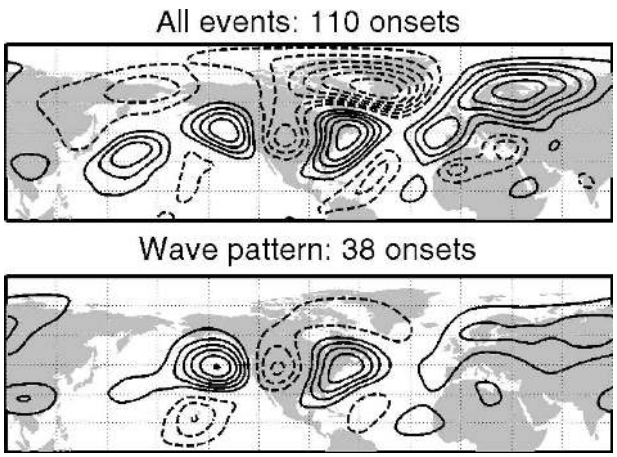

FIG. 14. (top) Composite of the 250-hPa streamfunction averaged from two to four days before the 110 Atlantic onset days. (bottom) The same composite, but only including events preceded by a wave train over North America. Note that the anomalies in this panel have been scaled by 38/110 to show their contribution to the overall anomalies. Contours are drawn every 1×10^6 s^{-1}; zero contour omitted.

train of anomalies stretching from the Pacific, across North America, and into the Atlantic.

To examine the effect of European blocking, the two-dimensional index was used to isolate those Atlantic episodes for which there was a blocking episode over at least one point in a European region (45°–65°N, 15°W–30°E) for all of two to four days prior to the onset date of the Atlantic event. This choice of region and time scale is arbitrary, but the result is largely insensitive to the exact choice of region. By this criteria 61 out of the 110 Atlantic onset events were preceded by European blocking, and compositing these cases, and the remaining 49, separately suggests that the European blocking cases have been successfully identified (not shown). In these cases the onset of a GBE is associated with wave breaking upstream of a preexisting European block, which acts to shift the blocking anomaly upstream (Tyrlis and Hoskins 2008a). The European block could be acting to increase the likelihood of wave breaking by imposing diffluent flow over the Atlantic, leading to meridionally elongated transient eddies, which favor wave breaking (e.g., Shutts 1983; Luo 2005).

We now identify those onset events that are preceded by a wave pattern across North America. To do this we define a daily index based on the normalized streamfunction anomalies at (45°N, 40°W), (45°N, 75°W), and (45°N, 105°W). If these anomalies are of the correct sign and greater than 2×10^6 m^2 s^{-1} in magnitude, then we define that day as exhibiting a North American wave pattern. We then identify GBE onset events for which the North American wave pattern is detected for

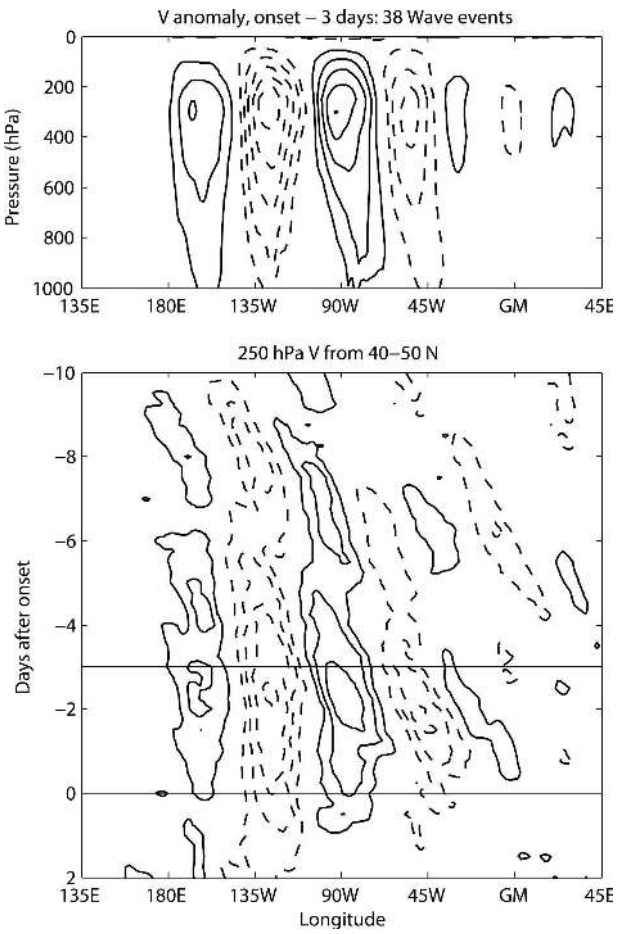

FIG. 15. (top) Cross section of the meridional wind anomalies at 45°N three days before onset averaged over the 38 events that show the North American wave train precursor. Contours are drawn every 3 m s^{-1}; negative contours dashed and zero contour omitted. (bottom) Hovmöller plot showing the time evolution of meridional wind anomalies averaged over 40°–50°N for the same events. Time runs in the direction of the negative y axis; contours are drawn every 4 m s^{-1} with negative contours dashed and zero contour omitted. The thin horizontal lines indicate onset day and day −3, when the vertical section was taken.

at least one day out of the four days leading up to the onset date.

In all, 38 out of the 110 onset events are considered to be preceded by the North American wave pattern under these criteria, and these are composited in the bottom panel of Fig. 14. This composite is dominated by the three midlatitude anomalies across North America and a tropical anomaly in the vicinity of Hawaii. The vertical structure of the wave train anomalies is illustrated in the top panel of Fig. 15, by compositing the meridional wind anomaly along 45°N three days before onset. The wind anomalies are deep, attain maximum amplitude at about 300 hPa, and are close to equivalent barotropic in structure. These features are

typical of stationary or quasi-stationary Rossby waves (e.g., Ambrizzi and Hoskins 1997).

The wave anomalies are seen to exist over a week before onset and drift eastward with a phase velocity of the order of just a few degrees per day, as shown in the bottom panel of Fig. 15 by a Hovmöller plot of the meridional wind at 250 hPa averaged over the latitude band 40°–50°N. Transient waves pass through the region, propagating with group velocities of around 30° day^{-1}. One of these in particular, appearing around six days before onset, is seen to interact with, and strengthen, the anomalies in the days leading up to onset. The onset itself occurs when the anticyclonic wave anomaly reaches the start of the Atlantic storm track, suggesting that in these cases wave breaking occurs through the interaction of the low-frequency anomalies and high-frequency transients. This is consistent with Feldstein (2003), who showed that both high- and low-frequency transient eddy fluxes contribute to the growth of NAO anomalies.

Finally, it should be noted that enhanced storm activity at the start of the Atlantic storm track is another clear precursor to wave breaking (Fig. 6). Developing storms clearly play a role in generating the cyclonic wind anomalies involved in the wave breaking, as suggested by Colucci (1985), Orlanski (2003), and Tyrlis and Hoskins (2008a).

b. Pacific events

Given that downstream blocking emerges as a frequent precursor to Atlantic wave breaking, we now examine the Pacific events for evidence that the same occurs here. As before, this is done by choosing an East Pacific region (45°–65°N, 120°–165°W) and defining this region as blocked whenever at least one point within it is considered part of a blocking episode, as identified by the two-dimensional wave-breaking index. If this occurs for all of two to four days before the onset date of a Pacific HLBE, downstream blocking is identified as a precursor. With these criteria, 99 out of the 105 Pacific onset events are preceded by east Pacific blocking, so this indeed emerges as a clear precursor. It is, in fact, the only consistent large-scale precursor seen in composites of the 250-hPa streamfunction (not shown). As in the Atlantic, there is unusually strong storm activity at the start of the storm track in the few days before onset, suggesting that developing storms also play a key role in generating the cyclonic winds involved in the wave breaking.

c. Lagged correlations between regions

Figure 2 shows that there is a change in HLBE frequency in the Pacific between positive and negative NAO months, and also a small change in the Atlantic associated with the WPP. This suggests that there is some connection between HLBEs in the two basins. Here we calculate lagged correlations between blocking activity in different regions to investigate any links. The time series used here are daily indicators of wave breaking, and can only take two values: one if there is a wave-breaking episode in a given region and zero if there is not. In each winter 90 days of data are selected for each series. For zero lag these days are 1 December–28 February, and for a 2-day lag, for example, one series will run from 31 November to 27 February, and the other will run from 2 December to 1 March. Statistical significance is estimated using a t test based on an effective sample size:

$$N_{\text{eff}} = N\left(\frac{1 - \rho_{1a}\rho_{1b}}{1 + \rho_{1a}\rho_{1b}}\right),$$

where N is the actual sample size and ρ_{1a} and ρ_{1b} are the lag-1 autocorrelation coefficients of the two time series. All correlations found are very small, as expected when using unfiltered daily data, but many values are statistically significant.

Correlations for lags of −40 to 40 days are shown in Fig. 16. The top panel shows correlations between GBEs and northern European blocking. There is a significant positive correlation for the European region leading the Atlantic by two days, supporting the finding that European blocking often acts as a precursor to Atlantic events. The bottom panel shows correlations between HLBEs in the Atlantic and Pacific sectors. Though there is a significant correlation at zero lag, the strongest correlations are seen with the Atlantic leading the Pacific by two to six days. This supports the notion that there is some connection between HLBEs in the two basins, but the mechanism behind this is unclear.

d. The effect of the stratosphere

Several studies have suggested that variability in the stratosphere could affect the NAO (e.g., Scaife et al. 2005), so it is of interest to look for a link between the stratosphere and the occurrence of GBEs. First, we define a daily time series of the stratospheric vortex strength as measured by the zonal mean wind at 50 hPa, 60°N. The series is normalized using the mean and standard deviation of the respective calendar day so that the seasonal cycle is removed. Lag correlations of this series with the Atlantic and Pacific HLBE series are shown in the bottom two panels of Fig. 16. In both basins there are significant negative correlations for the vortex leading the occurrence of HLBEs, by up to 20 days in the Pacific and out to 40 days in the Atlantic. In

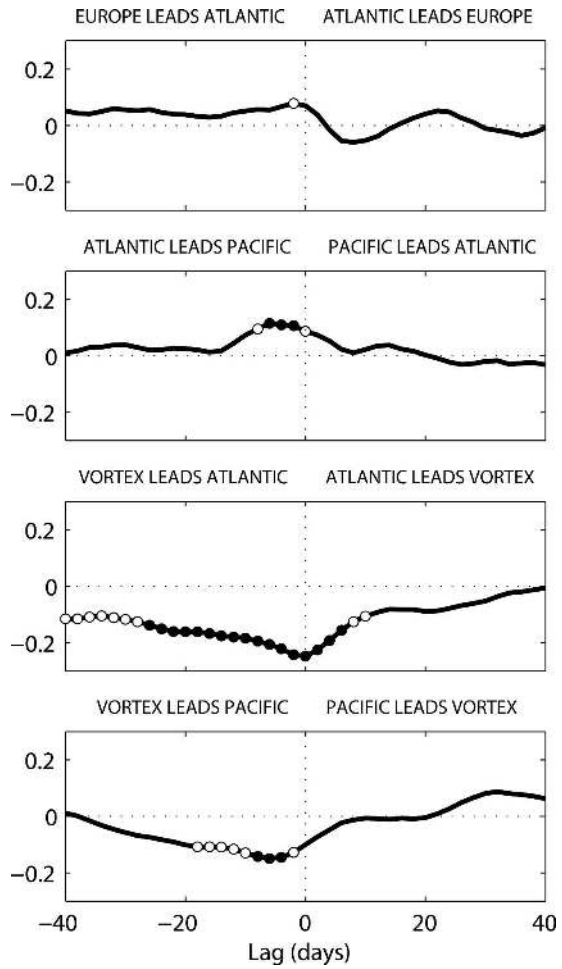

FIG. 16. Lagged correlations for daily winter indices of wave breaking over the Atlantic (50°–60°N, 30°–70°W), the Pacific (40°–50°N, 135°–175°E), and northern Europe (55°–65°N, 0°–30°E), and for the strength of the polar vortex as measured by the zonal mean wind at 60°N, 50 hPa. Points marked with an open circle are significant at the 95% level; those marked with filled circles, at the 99% level.

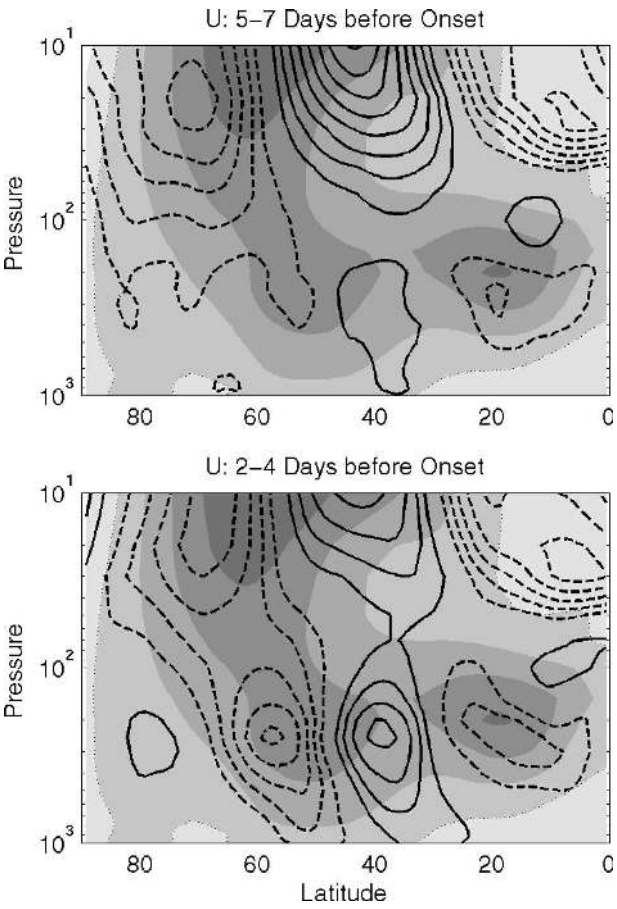

FIG. 17. Composites of the zonal wind averaged over the Atlantic sector (0°–60°W) in periods prior to the onset of GBEs. These are shown as anomalies from the mean of all non-GBE days, which is shaded at 10 m s^{-1} intervals. Anomalies are contoured every 0.5 m s^{-1}, negative contours dashed, and zero contour omitted.

the Atlantic there are also significant negative correlations with Atlantic HLBEs leading the vortex by up to 10 days. This difference in time scale, and the sign of correlation, are consistent with the troposphere–stratosphere NAO relationship seen by Ambaum and Hoskins (2002). These correlations show that there is potentially some predictability of the occurrence of high-latitude blocking to be gained from knowledge of the state of the stratosphere, though as before the correlations, and hence the fraction of variance accounted for, are small.

Further insight into the stratospheric influence on the NAO is given by compositing the zonal wind, averaged over the Atlantic basin, in the period before the onset of GBEs. These composites are shown in Fig. 17 as anomalies from the mean non-GBE, or basic state as shown in Fig. 12, in order to determine whether, among all non-GBE days, these days exhibit anomalies that make a GBE more likely to occur. If these composites are plotted as anomalies from the full climatology instead, the anomaly patterns are dominated by the differences between the two states in Fig. 12. An equatorward shift in the stratospheric jet is apparent about a week before onset, and a similar shift in the tropospheric eddy-driven jet is seen a few days later. This suggests that wave breaking is more likely to occur when the eddy-driven jet is shifted toward the equator, perhaps because the region of ambient cyclonic shear on the poleward side of the jet is then more closely aligned with the low-level baroclinic zone. This is in line with the finding of Tyrlis and Hoskins (2008b) that the direction of wave breaking is largely determined by the background shear. It appears that such a shift in the

TABLE 1. Total number of onset events in each 22-winter half of ERA-40 and the number of events for which each of the three large-scale precursors were identified.

Period	Total onsets	European blocking	Wave train	Stratospheric jet shift
1957/58–1978/79	59	35	19	2
1979/80–2000/01	50	25	18	14

tropospheric eddy-driven jet can occur in response to a similar shift in the stratospheric jet.

e. Relevance to the NAO trend

The ERA-40 period coincides with a marked upward trend of the NAO index from very low negative values in the 1960s to high positive values in the 1990s (though note that the index has since fallen to near zero). Figure 11 shows that this trend is associated with a decrease in the occurrence of GBEs, so it is clearly of interest to see whether this decrease could be linked to a reduction in the occurrence of a particular precursor.

To examine this, the ERA-40 period was divided into two halves of 22 complete winters each, namely 1957/58–1978/79 and 1979/80–2000/01. Note that in doing this, one onset date in December 2001 is ignored, so there are only 109 onsets in total. The European blocking and wave train precursors were identified as before, and events preceded by a shift in the stratospheric vortex were found using the following method. First, the zonal wind at 10 hPa was averaged over the Atlantic sector 0°–60°W and over two to four days before each onset date. If this average wind strength was found to be greater than half a standard deviation above the mean at 40°N and less than half a standard deviation below the mean at 70°N, then the onset event was considered to be preceded by a shift in the stratospheric jet.

For each period, the total number of onset events and the number for which each precursor is identified is given in Table 1. There are fewer onset events in the second half of ERA-40 than the first, consistent with the trend in the NAO index. There is a dramatic difference between the two halves in the number of stratospheric jet shift events. However, this change is of the wrong sign to be linked to a positive NAO trend, and is most likely a reflection of the quality of the analyzed stratospheric variability in the first half of ERA-40 when little or no satellite data was available. There is no significant change in the number of wave train events between the two periods, but there is a clear change in the number of European blocking events. This is of the correct sign and magnitude to account for the change in the total number of onset events, suggesting that the NAO trend could be linked to a reduction in the European blocking precursor. This is consistent with the impression that the strongly negative NAO in the 1960s was associated with the unusually cold winters experienced in Europe at the time due to a spate of European blocking activity.

8. Discussion

The NAO is essentially a measure of the variability of the zonal flow over the Atlantic basin. We have presented strong evidence in this paper to support the hypothesis that, on interannual and longer time scales, this variability is a result of variations in the occurrence of high-latitude blocking. The negative NAO is a description of periods when high-latitude blocking is frequent, so the zonal flow is weak on average. The positive NAO is simply a description of periods when it occurs infrequently, so the zonal flow is therefore strong. A similar, albeit weaker, relationship exists between the WPP and high-latitude blocking over the Pacific.

In this view of the NAO there are only two distinct states, namely a basic state and a blocked state. This is in contrast to the synoptic view of the NAO proposed by Benedict et al. (2004), who consider the positive phase of the NAO as a distinct state resulting from two anticyclonic wave-breaking events: one over the west coast of North America and one over the subtropical North Atlantic. Our two-dimensional index does not give any indication that wave-breaking events at such low latitudes are related to the NAO, though it does show a region of increased blocking centered over Spain during positive NAO months (Fig. 2). Composites of these events (not shown) do resemble positive NAO anomalies, but they are shifted to the north with a high pressure center level with the southern tip of the United Kingdom, as would be expected from a reversal of the gradient over Spain. If we take the same approach as in Fig. 9 and remove the influence of blocking over Spain from the positive NAO months, then we are still left with a clear positive NAO anomaly pattern. We therefore suggest that the signal over Spain in Fig. 2 largely reflects variations in central European blocking as a result of NAO variability.

The absence of anticyclonic wave breaking in our results could be due to the time and space scales prescribed, which prevent the identification of more transient events. As described by Vallis and Gerber (2007, manuscript submitted to *Dyn. Atmos. Oceans*), anticyclonic wave breaking on the equatorward side of the jet could be interpreted as acting to shift the jet poleward of its climatological position. However, if these events

are more transient, they could be signatures of conventional LC1-type cyclones (Thorncroft et al. 1993) driving a strong subpolar jet, which could be interpreted as part of the basic state suggested here. It is also worth noting that in this basic, or positive NAO, state the entrance of the subtropical jet over the Atlantic lies southwest of the subpolar jet exit, which is in the vicinity of northern Europe. A potential temperature contour following the axes of both jets will thus overturn in a manner resembling wave breaking.

The relationship between subtropical anticyclonic wave breaking and the NAO clearly deserves further attention in future work. Here, we simply note that we do not need to consider these events in order to explain the low-frequency variability associated with the NAO. Such events may have an effect of course, for example, as a positive feedback to increase the zonal wind speeds during periods characterized by the positive NAO, as suggested by Abatzoglou and Magnusdottir (2006).

This leads to the issue of feedbacks in general. To what extent does a count of HLBE days, as in Fig. 11, equate to a count of synoptic events, or is it rather a measure of the predominance of a certain "regime"? Manual inspection reveals that high-latitude blocking episodes are initiated and maintained in the same way as conventional midlatitude blocking (e.g., Hoskins and Sardeshmukh 1987). Onset is achieved via an upper-level wave-breaking event, and then the situation is maintained by subsequent wave-breaking events associated with synoptic storms passing to the south. While the situation may appear static in surface pressure for example, these subsequent wave-breaking events often result in a complete replacement of the original anticyclonic air mass. This supports our view of the NAO as describing low-frequency variations in the occurrence of synoptic events, but also highlights the potential importance of feedback where the high-latitude blocking situation increases the likelihood of subsequent wave-breaking events, which in turn act to maintain the blocking. Eddy feedback could also play a role in the maintenance of both basic and blocked states via the action of synoptic eddies to reinforce the current position of the jet.

The focus of this paper has been to understand the low-frequency variability of the NAO, so we have used monthly and seasonal mean data to identify the NAO. Given the synoptic nature of this interpretation, it is natural to ask how much of the variability on shorter time scales can also be explained by GBEs. To look at this we use the daily NAO index calculated by the NOAA Climate Prediction Center using least squares regression onto the monthly teleconnection patterns. Figure 18 shows lagged correlations of the winter daily

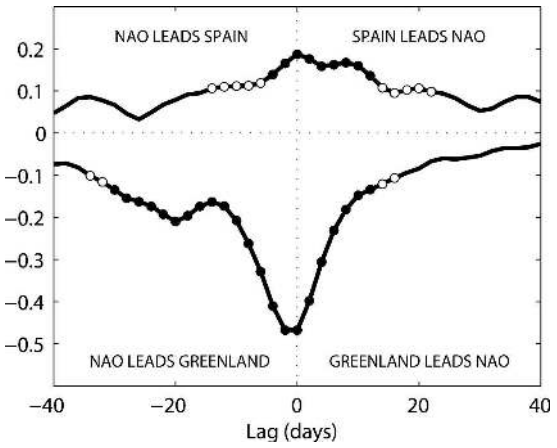

FIG. 18. Lagged correlations of the daily NAO index with blocking over Spain (35°–45°N, 20°W–20°E; positive correlations) and GBEs (negative correlations).

NAO index with GBE activity. This shows a simultaneous correlation between the two time series of −0.47, a large value to obtain from unfiltered daily data, especially considering that the GBE series is binomial and has a threshold of five days in the definition of an episode. GBEs clearly make a large contribution to the variability seen in the daily NAO index, as expected from the composites shown in section 4. However, it is also possible that on short time scales the NAO index can be influenced by other factors, perhaps the exact strength or location of the jet when zonal flow prevails. These could be essentially random synoptic variations that average out over periods of a few years or longer.

An interesting feature of Fig. 18 is the "shoulder" of high correlations with the NAO leading by 10–20 days. This may be a reflection of the stratospheric influence, as described by Ambaum and Hoskins (2002), but this has not been investigated further. Also shown in Fig. 18 is the correlation with blocking activity in the region over Spain, as discussed above. This yields much weaker correlations with the NAO, consistent with the suggestion above that this is a much weaker relationship than that between GBEs and the NAO.

This study is complementary to that of Tyrlis and Hoskins (2008b), who apply the one-dimensional blocking index of Pelly and Hoskins (2003) to the ERA-40 dataset. The one-dimensional index only searches for wave-breaking events along the storm track axis, so the events identified do act to block the westerlies and the storm track and, thus, can be considered blocking events in the traditional sense. Many of the high-latitude blocking episodes studied here are not identified as blocking events by the one-dimensional index. However, the classical blocking events alone do not explain the variability of the NAO: if we use the

two-dimensional index but restrict the Atlantic region to 49°N, 30°–70°W (approximately the "central blocking latitude" used by the one-dimensional index over the western Atlantic), the correlation of GBE occurrence with the NAO drops from 0.84 to 0.55.

The NAO is closely related to a pattern referred to as the "Northern Annular Mode" (NAM), which emerges as the leading EOF of Northern Hemisphere MSLP (Thompson and Wallace 2000). Here we have focused exclusively on the NAO, but the same mechanisms are clearly relevant to explaining both patterns. Several studies have attributed variations of the NAM, and its Southern Hemisphere counterpart, to transient eddy fluxes of momentum (Thompson et al. 2002) or PV (Goodman and Czaja 2007, manuscript submitted to *Quart. J. Roy. Meteor. Soc.*). This is consistent with the hypothesis presented here, since wave breaking involves the large-scale advection of subtropical air to high latitudes and polar air toward the equator, and these will be identified as large transient eddy fluxes by such analyses.

To conclude, we have presented a new interpretation of the winter NAO as a description of variations in the occurrence of high-latitude blocking episodes resulting from Rossby wave–breaking events. Several dynamical precursors to wave breaking have been identified, including downstream blocking and an enhanced storm track. They also include a quasi-stationary Rossby wave train stretching across North America from the Pacific. This opens up a potential mechanism by which variability in the tropical Pacific could affect the NAO, as has been suggested by Hoerling et al. (2001), Lin et al. (2005), and Kucharski et al. (2006). There is also evidence that variability of the stratospheric polar vortex can influence the occurrence of tropospheric wave breaking, in line with the evidence presented by Scaife et al. (2005) and Wittman et al. (2007).

This new interpretation provides an attractively simple understanding of the NAO response to forcing. External forcings can be viewed as having a direct effect, which adjusts the basic state in some way, and an indirect "NAO response" if this new state is more, or less, conducive to the occurrence of wave breaking or if the preferred location of wave breaking is altered. Such responses occur in the experiments of Deser et al. (2004) and in the shift of the NAO pattern seen by Ulbrich and Cristoph (1999).

Acknowledgments. We are grateful to ECMWF and BADC for providing the data, to the reviewers for constructive comments, and to Evangelos Tyrlis and Maarten Ambaum for useful discussions. TJW was supported by a NERC RAPID grant.

REFERENCES

Abatzoglou, J. T., and G. Magnusdottir, 2006: Opposing effects of reflective and nonreflective planetary wave breaking on the NAO. *J. Atmos. Sci.,* **63,** 3448–3457.

Ambaum, M. H. P., and B. J. Hoskins, 2002: The NAO troposphere–stratosphere connection. *J. Climate,* **15,** 1969–1978.

Ambrizzi, T., and B. J. Hoskins, 1997: Stationary Rossby-wave propagation in a baroclinic atmosphere. *Quart. J. Roy. Meteor. Soc.,* **123,** 919–928.

Barriopedro, D., R. García-Herrera, A. R. Lupo, and E. Hernández, 2006: A climatology of Northern Hemisphere blocking. *J. Climate,* **19,** 1042–1063.

Benedict, J. J., S. Lee, and S. B. Feldstein, 2004: Synoptic view of the North Atlantic Oscillation. *J. Atmos. Sci.,* **61,** 121–144.

Berrisford, P., B. J. Hoskins, and E. Tyrlis, 2007: Blocking and Rossby wave breaking on the dynamical tropopause in the Southern Hemisphere. *J. Atmos. Sci.,* **64,** 2881–2898.

Cheng, X., and J. M. Wallace, 1993: Cluster analysis of the Northern Hemisphere wintertime 500-hPa height field: Spatial patterns. *J. Atmos. Sci.,* **50,** 2674–2696.

Colucci, S. J., 1985: Explosive cyclogenesis and large-scale circulation changes: Implications for atmospheric blocking. *J. Atmos. Sci.,* **42,** 2701–2717.

Croci-Maspoli, M., C. Schwierz, and H. Davies, 2007: Atmospheric blocking: Space-time links to the NAO and PNA. *Climate Dyn.,* **29,** 713–725.

Deser, C., G. Magnusdottir, R. Saravanan, and A. Phillips, 2004: The effects of North Atlantic SST and sea ice anomalies on the winter circulation in CCM3. Part II: Direct and indirect components of the response. *J. Climate,* **17,** 877–889.

Diao, Y., J. Li, and D. Luo, 2006: A new blocking index and its application: Blocking action in the Northern Hemisphere. *J. Climate,* **19,** 4819–4839.

Feldstein, S. B., 2003: The dynamics of NAO teleconnection pattern growth and decay. *Quart. J. Roy. Meteor. Soc.,* **129,** 901–924.

Franzke, C., S. Lee, and S. B. Feldstein, 2004: Is the North Atlantic Oscillation a breaking wave? *J. Atmos. Sci.,* **61,** 145–160.

Hoerling, M. P., J. W. Hurrell, and T. Xu, 2001: Tropical origins for recent North Atlantic climate change. *Science,* **292,** 90–92.

Hoskins, B. J., and P. D. Sardeshmukh, 1987: A diagnostic study of the dynamics of the Northern Hemisphere winter of 1985–86. *Quart. J. Roy. Meteor. Soc.,* **113,** 759–778.

Huang, J., M. Ji, K. Higuchi, and A. Shabbar, 2006: Temporal structures of the North Atlantic Oscillation and its impact on the regional climate variability. *Adv. Atmos. Sci.,* **23,** 23–32.

Hurrell, J. W., 1995: Decadal trends in the North Atlantic Oscillation: Regional temperatures and precipitation. *Science,* **269,** 676–679.

Kimoto, M., and M. Ghil, 1993: Multiple flow regimes in the Northern Hemisphere winter. Part I: Methodology and hemispheric regimes. *J. Atmos. Sci.,* **50,** 2625–2643.

Kucharski, F., F. Molteni, and A. Bracco, 2006: Decadal interactions between the western tropical Pacific and the North Atlantic Oscillation. *Climate Dyn.,* **26,** 79–91.

Lin, H., J. Derome, and G. Brunet, 2005: Tropical Pacific link to the two dominant patterns of atmospheric variability. *Geophys. Res. Lett.,* **32,** L03801, doi:10.1029/2004GL021495.

Löptien, U., and E. Ruprecht, 2005: Effect of synoptic systems on the variability of the North Atlantic Oscillation. *Mon. Wea. Rev.,* **133,** 2894–2904.

Luo, D., 2005: Why is the North Atlantic block more frequent and long-lived during the negative NAO phase? *Geophys. Res. Lett.,* **32,** L20804, doi:10.1029/2005GL022927.

——, A. R. Lupo, and H. Wan, 2007: Dynamics of eddy-driven low-frequency dipole modes. Part I: A simple model of North Atlantic Oscillations. *J. Atmos. Sci.,* **64,** 3–28.

Orlanski, I., 2003: Bifurcation in eddy life cycles: Implications for storm track variability. *J. Atmos. Sci.,* **60,** 993–1023.

Pelly, J. L., and B. J. Hoskins, 2003: A new perspective on blocking. *J. Atmos. Sci.,* **60,** 743–755.

Rogers, J. C., 1981: The North Pacific Oscillation. *Int. J. Climatol.,* **1,** 39–57.

Scaife, A. A., J. R. Knight, G. K. Vallis, and C. K. Folland, 2005: A stratospheric influence on the winter NAO and North Atlantic surface climate. *Geophys. Res. Lett.,* **32,** L18715, doi:10.1029/2005GL023226.

Scherrer, S. C., M. Croci-Maspoli, C. Schwierz, and C. Appenzeller, 2006: Two-dimensional indices of atmospheric blocking and their statistical relationship with winter climate patterns in the Euro-Atlantic region. *Int. J. Climatol.,* **26,** 233–249.

Schwierz, C., M. Croci-Maspoli, and H. C. Davies, 2004: Perspicacious indicators of atmospheric blocking. *Geophys. Res. Lett.,* **31,** L06125, doi:10.1029/2003GL019341.

Shabbar, A., J. Huang, and K. Higuchi, 2001: The relationship between the wintertime North Atlantic Oscillation and blocking episodes in the North Atlantic. *Int. J. Climatol.,* **21,** 355–369.

Shutts, G. J., 1983: The propagation of eddies in diffluent jetstreams: Eddy vorticity forcing of 'blocking' flow fields. *Quart. J. Roy. Meteor. Soc.,* **109,** 737–761.

Thompson, D. W. J., and J. M. Wallace, 2000: Annular modes in the extratropical circulation. Part I: Month-to-month variability. *J. Climate,* **13,** 1000–1016.

——, S. Lee, and M. P. Baldwin, 2002: Atmospheric processes governing the Northern Hemisphere Annular Mode/North Atlantic Oscillation. *The North Atlantic Oscillation: Climatic Significance and Environmental Impact, Geophys. Monogr.,* Vol. 134, Amer. Geophys. Union, 81–112.

Thorncroft, C. D., B. J. Hoskins, and M. E. McIntyre, 1993: Two paradigms of baroclinic-wave life-cycle behaviour. *Quart. J. Roy. Meteor. Soc.,* **119,** 17–55.

Tibaldi, S., and F. Molteni, 1990: On the operational predictability of blocking. *Tellus,* **42A,** 343–365.

Tyrlis, E., and B. J. Hoskins, 2008a: Aspects of Northern Hemisphere atmospheric blocking climatology. *J. Atmos. Sci.,* in press.

——, and ——, 2008b: The morphology of Northern Hemisphere blocking. *J. Atmos. Sci.,* in press.

Ulbrich, U., and M. Cristoph, 1999: A shift of the NAO and increasing storm track activity over Europe due to anthropogenic greenhouse gas forcing. *Climate Dyn.,* **15,** 551–559.

Uppala, S. M., and Coauthors, 2005: The ERA-40 re-analysis. *Quart. J. Roy. Meteor. Soc.,* **131,** 2961–3012.

Vallis, G. K., and E. Gerber, 2007: Local and hemispheric dynamics of the North Atlantic Oscillation, annular patterns and the Zonal Index. *Dyn. Atmos. Oceans,* in press.

——, E. P. Gerber, P. J. Kushner, and B. A. Cash, 2004: A mechanism and simple dynamical model of the North Atlantic Oscillation and annular modes. *J. Atmos. Sci.,* **61,** 264–280.

van Loon, H., and J. C. Rogers, 1978: The seesaw in winter temperatures between Greenland and Northern Europe. Part I: General description. *Mon. Wea. Rev.,* **106,** 296–310.

Vautard, R., 1990: Multiple weather regimes over the North Atlantic: Analysis of precursors and successors. *Mon. Wea. Rev.,* **118,** 2056–2081.

Wallace, J. M., and D. S. Gutzler, 1981: Teleconnections in the geopotential height field during the Northern Hemisphere winter. *Mon. Wea. Rev.,* **109,** 784–812.

Wanner, H., S. Brönnimann, C. Casty, D. Gyalistras, J. Luterbacher, C. Schmutz, D. B. Stephenson, and E. Xoplaki, 2001: North Atlantic Oscillation—Concepts and studies. *Surv. Geophys.,* **22,** 321–381.

Wittman, M. A. H., A. J. Charlton, and L. M. Polvani, 2007: The effect of lower stratospheric shear on baroclinic instability. *J. Atmos. Sci.,* **64,** 479–496.